Journal of Alloys and Compounds 505 (2010) 319–323

Contents lists available at ScienceDirect

Journal of Alloys and Compounds

journal homepage: www.elsevier.com/locate/jallcom

Effect of cryogenic treatment on microstructure and mechanical behaviors of the Cu-based bulk metallic glass matrix composite

Guozhi Ma, Ding Chen*, Zhenhua Chen, Wei Li

School of Materials Science and Engineering, Hunan University, Changsha 410082, PR China

ARTICLE INFO

Article history:
Received 27 January 2010
Received in revised form 2 June 2010
Accepted 10 June 2010
Available online 17 June 2010

Keywords:
Cu-based bulk metallic glass composite
Cryogenic treatment
Martensite
Fracture

ABSTRACT

Effect of cryogenic treatment (CT) on microstructure and mechanical properties of the Cu-based bulk metallic glasses matrix composite ($Cu_{46}Zr_{46}Al_8$) was investigated. CT brought about the refinement of the primary CuZr phase, the formation of the martensite phase accompanying with the morphology modification of the CuZr precipitates, contributing to the improvement in the microhardness and the compression fracture strength. The size of the CuZr crystalline phase was reduced from about 3 μm to 2 μm and the morphology of the CuZr precipitate was transformed from the rotundity to the short rod-shape. The compression fracture strength and the microhardness of the as-cast $Cu_{46}Zr_{46}Al_8$ composite were 1340 MPa and 512 Hv respectively, while they were 1759 Mpa and 574 Hv respectively after CT. Furthermore, CT accelerated the fracture morphology transformation from the ductile to the brittle. The possible mechanisms involved in microstructural modification and strength as well as microhardness improvement were discussed.

1. Introduction

The recent findings of the bulk glass forming alloys have received much attention and are promising for the further development of the bulk metallic glasses (BMGs) with the potential technological applications [1]. However, the monolithic BMGs usually exhibit poor plasticity and no stain hardening ability during deformation at the ambient temperatures due to the highly localized shear bands, which significantly limits the range of possible applications [2]. In the past decades, continuous attempts have been made to enhance the ductility of the multi-component BMGs through designing a composite microstructure. Usually, two processing are adopted to prepare the glass matrix based composites. One is the controllable annealing treatment of the amorphous precursor, while the other is the ex situ or in situ formation of the composite. Up to now, the rather high plasticity of the amorphous alloys can be achieved by partial crystallization [3–5].

The Cu-based BMGs have attracted the increasing interests due to their good glass forming ability (GFA), ultrahigh strength and rather low cost [6,7]. In the recent years, some studies have been conducted on improving the GFA and mechanical properties of the $(Cu_{50}Zr_{50})_{100-x}Al_x$ BMG and BMG matrix composites [6–8]. Cheung and Shek [7] found that the ΔT_x was optimized at 73 K and the alloy exhibited the highest thermal stability with the Al content of 8 at.%. In addition, Yu et al. found that the alloy containing 8% Al exhibited the best GFA in the alloy series and the amorphous rod with the diameter over 5 mm was obtained [9]. Therefore, the $Cu_{46}Zr_{46}Al_8$ alloy was selected in the present study. The $Cu_{46}Zr_{46}Al_8$ composite was prepared at the given cooling rate and then experienced CT. CT is a novel way to modify the microstructure and mechanical properties of metallic materials. Most studies have been focused on their deformation behaviors during cryogenic temperature, while few investigations have been conducted on the mechanical properties of BMG and BMGC after CT. To achieve wider applications in space exploration and liquefied gas storage, it is important to study the mechanical properties of the BMG and BMGC at the cryogenic temperature and after CT [10].

The present work aims to study the effect of the CT on the microstructure and mechanical properties of the Cu-based bulk metallic glasses matrix composite and try to identify the different fracture features from the morphology.

2. Experimental

The $(Cu_{50}Zr_{50})_{92}Al_8$ glass matrix composite was prepared by arc melting mixtures of Cu, Zr and Al with the purities higher than 99.9% in a Zr-gettered argon atmosphere. The alloy ingots were repeatedly melted four times to ensure composition homogeneity and then was suction cast into a copper mold to form cylindrical rods with 4 mm in diameter. Some samples were then treated by cryogenic processing. The samples were immersed into liquid N_2 namely CT for 4 h, 24 h, 60 h and 72 h, respectively.

The microstructure was investigated by X-ray diffraction (XRD) with the Cu *K* radiation, the optical microscopy (OM, Leitz-MM6) and scanning electronic microscopy (SEM, JSM-6700F) at the same location before and after CT. The specimens for mechanical testing were cut from the rods with the height and the diameter

* Corresponding author. Tel.: +86 731 8821648; fax: +86 731 8821648.
E-mail address: ma97chen@hotamil.com (D. Chen).

0925-8388/$ – see front matter © 2010 Published by Elsevier B.V.
doi:10.1016/j.jallcom.2010.06.063

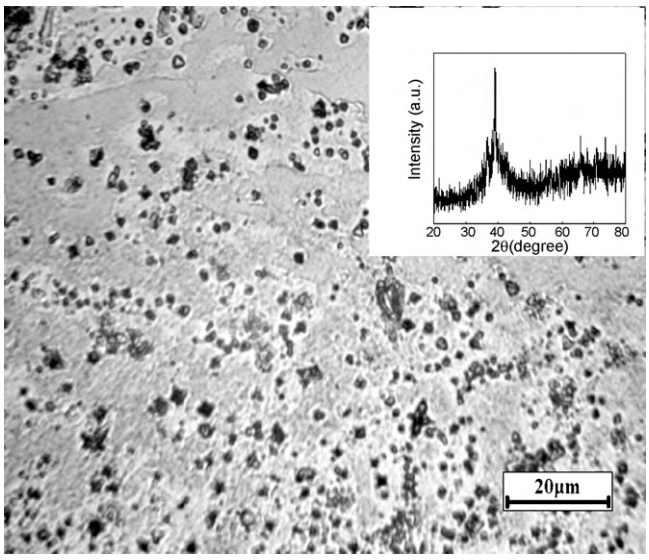

Fig. 1. The optical micrograph and the XRD pattern of the as-cast $Cu_{46}Zr_{46}Al_8$ composite.

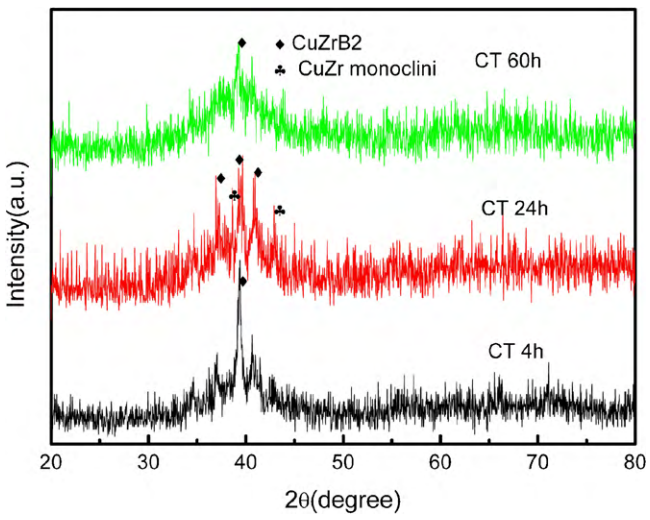

Fig. 3. The XRD patterns of the $Cu_{46}Zr_{46}Al_8$ composites after CT.

of 8 mm and 4 mm respectively. They were grounded and polished prior to testing. The hardness testing was conducted on a HBRVU-187.5 hardness tester under a load of 200 g and a holding time of 15 s. The microhardness value was averaged from seven points on each sample and the error was below 10. The compressive tests were conducted on a quasi-static loading apparatus at an initial strain rate of $5 \times 10^{-4}\ s^{-1}$. The compressive strength was averaged from three samples and the error was not beyond 15. The compression fracture surfaces were examined by SEM.

3. Results and discussion

The optical micrograph and the XRD pattern of the as-cast $Cu_{46}Zr_{46}Al_8$ composite are shown in Fig. 1. As indicated by the XRD pattern, the visible crystalline peaks corresponding to the CuZr crystalline phase (Pdf #49-1483) was detected, which was in accordance with the literature [11]. The CuZr crystalline phase was in the form of rotundity and was mainly located in the amorphous area. Most of the CuZr particles were about 3 μm in size and were homogeneously dispersed in the glassy matrix, while only a small fraction of them were agglomerated locally.

Fig. 2 shows the optical micrographs of the $Cu_{46}Zr_{46}Al_8$ composite experienced CT. Obviously, the significant microstructural changes occurred after CT. As seen from Fig. 2a, the rotundity grains with the different sizes were existent in the amorphous matrix after CT for 4 h and the average size of the particles was about 2 μm, smaller than those in the as-cast sample. As seen from Fig. 2b, the crystalline phase was transformed from the rotundity to the short rod-shape after CT for 24 h and its average size was still much

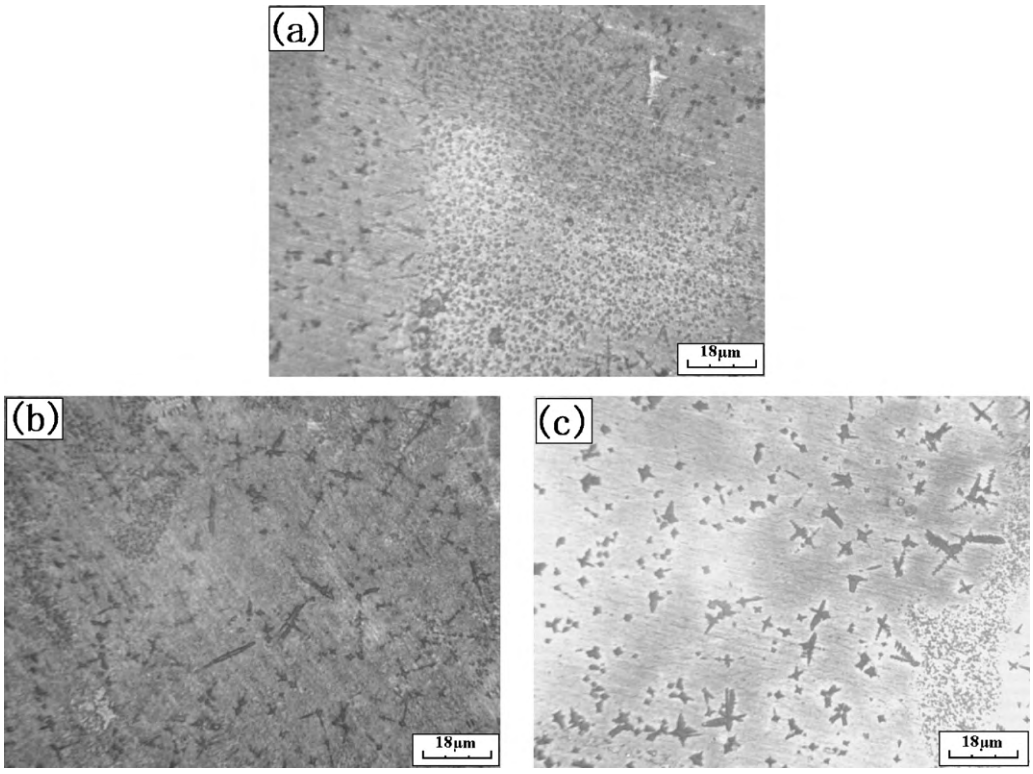

Fig. 2. Optical micrographs of the $Cu_{46}Zr_{46}Al_8$ composite after CT (a) CT for 4 h; (b) CT for 24 h; (c) CT for 60 h.

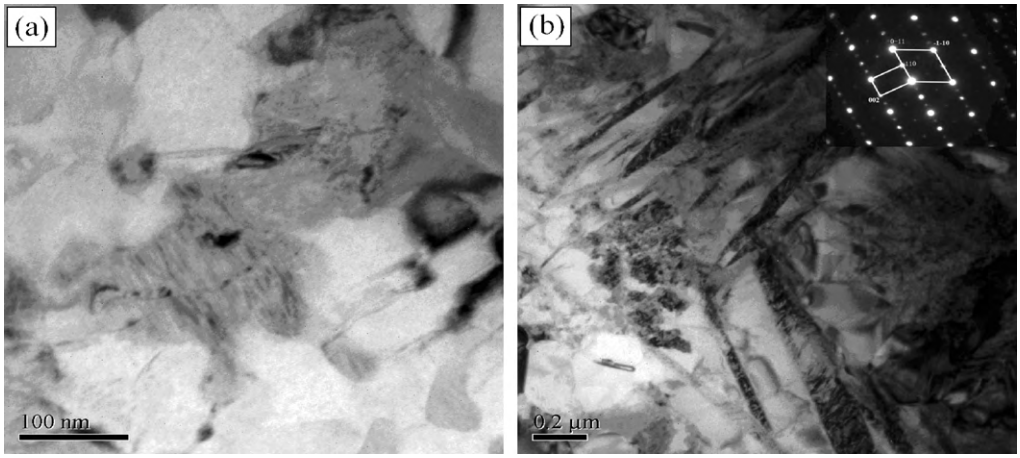

Fig. 4. TEM image of the $Cu_{46}Zr_{46}Al_8$ samples (a) before CT and (b) after CT.

smaller than that in the as-cast. Furthermore, as indicated by Fig. 2c, there were three morphologies of the crystalline phase, i.e. rotundity, short rod-shape and dendrite for the as-cast samples after CT for 60 h and its distribution was more homogenous than that in the as-cast.

The XRD patterns of the $Cu_{46}Zr_{46}Al_8$ composite after CT are shown in Fig. 3. As seen from Fig. 3, more crystalline peaks except the general CuZr phase were observed after CT for 24 h. The extra crystalline peaks were mainly identified as the monoclinic CuZr phase (Pdf#49-1485).

It was reported that an interesting phenomenon such as a martensitic transformation from the cubic primitive B2 (Pm-3m) to the monoclinic B19′ (P21/m and Cm) phase was existent in the Cu–Zr-based alloys [12–14]. The microstructural observation indicated that a martensitic transformation probably occurred during the CT for 24 h (as seen in Fig. 3). However, the crystalline CuZr phase exists in a wide variety of morphologies and microstructures [14]. Although the alloy composition is similar, the morphologies of the CuZr intermetallic compound (either B2 parent phase or monoclinic martensite phase) are rather diverse in different alloys system

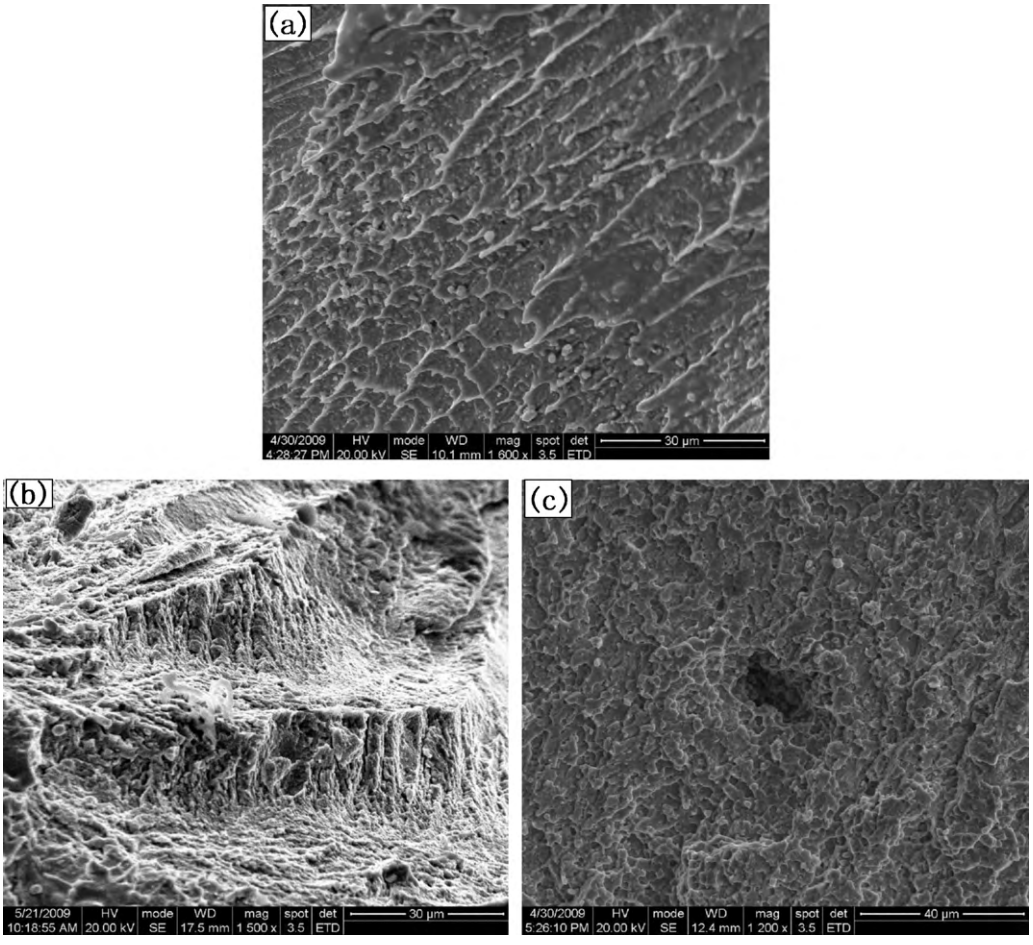

Fig. 5. The SEM fracture images of the $Cu_{46}Zr_{46}Al_8$ composites after different treatments (a) as-cast; (b) CT for 4 h; (c) CT for 24 h.

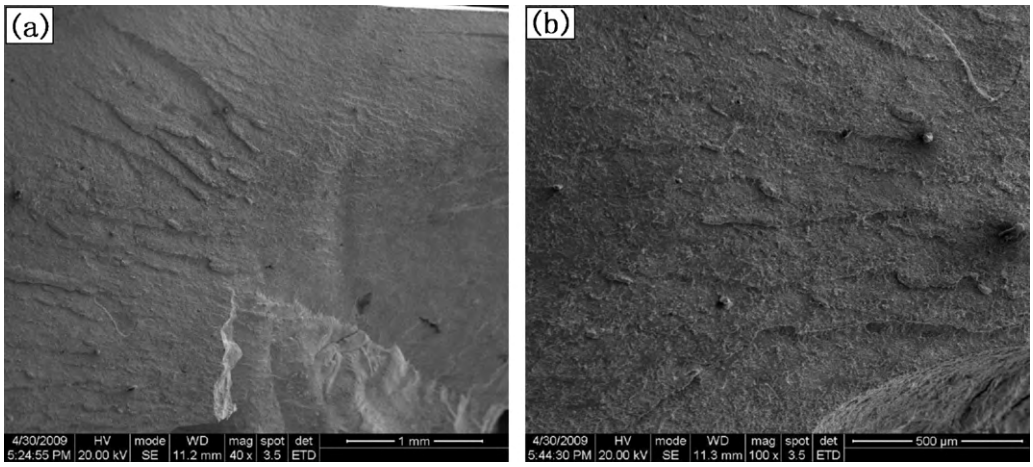

Fig. 6. The fracture surfaces of the sample experienced CT for 24 h.

or with the different cooling rates, ranging from the micrometer-sized dendrite in the slowly solidified alloy to the nanometer-sized particles formed with the high cooling rate. Therefore, TEM examination was conducted to identify the martensitic phase.

The TEM bright field images of the $Cu_{46}Zr_{46}Al_8$ samples before and after CT are shown in Fig. 4. As shown in Fig. 4a, the as-cast sample exhibited a mixed structure, i.e. the amorphous phase, the partial crystalline and the fully crystalline phase. Obviously, the cooling rate is not sufficient to prevent partial crystallization of the melt. At first the B2 CuZr phase precipitates and the remaining melt solidifies into a glass. It is well known that the growth of the CuZr intermetallic compound is rather fast [14]. Once the cooling rate drops to a critical degree during the solidification process, the CuZr phase instead of the amorphous phase will nucleate at the L/S interface and subsequently grow at a high rate. The solute redistribution in the remaining liquid thus results in the no longer formation of the amorphous phase.

As shown in Fig. 4b, the CT sample revealed the strip-like phase with several hundreds of nanometer in length and 5–10 nm in width. From the corresponding SAED pattern inserted in Fig. 4b, the crystalline phase was composed of the cubic primitive structure B2 CuZr phase and the monoclinic martensitic B19′ CuZr phase, which was consistent with the XRD results. Furthermore, the superlattice was also observed in the SAED pattern of the CT sample. It is known that there are two kinds of martensites found in the CuZr intermetallic compound, i.e. the normal martensite and the superlattice of the former [15]. As indicated by the weak points in the SAED pattern inserted in the Fig. 4b, the superlattice may be corresponding to the superstructure of the normal martensites.

The mechanical properties of the composite in the different states were summarized in the Table 1. The maximum of the microhardness and the compression strength were 574 Hv and 1759 MPa respectively after CT for 24 h. In addition, the maximum compressive fracture strength and the microhardness increased with the increase of the CT time. Due to the intrinsic brittle nature of the composite, almost zero plastic strain was existent after CT, which was in good agreement with the literatures that the plasticity of the BMG at cryogenic temperature was not distinctly improved but albeit certain increase in strength was found [16–19]. Therefore, the data of the compression yield strength were the same as those of the compression fracture strength. However, the intrinsic brittleness of the $Cu_{46}Zr_{46}Al_8$ composite was aggravated, which was indicated by Figs. 5 and 6.

Table 1
Microhardness and compression strength of the composites after CT.

Processing parameter	Mechanical properties at room temperature		
	Microhardness, Hv	Compression yield strength σ_y, MPa	Compression fracture strength σ_f, MPa
CT 0 h	512	1340	1340
CT 4 h	520	1476	1476
CT 24 h	574	1759	1759

The fracture images of the composite after CT are shown in Fig. 5. As shown in Fig. 5a, the as-cast composite exhibited a vein-like fracture pattern typical of the other metallic glasses [20–24]. Furthermore, the arrangement of the veins was in agreement with the flow direction in the shear plane, which was consistent with the previous literatures [25,26]. As shown in Fig. 5b, there was a sharp discontinuity between the fine striations and the intermittent smooth regions in the form of transversal steps for the sample experienced CT for 4 h, which indicated that the fracture occurred on a coarse plane after CT. The analogous morphologies of transversal steps were obtained in the different testing conditions and were observed on the fracture surface of a Zr-based amorphous alloy at high temperature [27]. As shown in Fig. 6c, the total brittle failure feature was observed for the sample experienced CT for 24 h, indicating that the CT accelerated the brittleness transition.

The fracture process of the sample experienced CT for 24 h is shown in Fig. 6. Fracture propagation was initiated with a few vein patterns and then continued to a zone in which cracks and mircovoids were formed, indicating micro-cracks joined together to form continuous cracks and then led to the final brittle fracture during the compression loading. Therefore, the plastic deformation ability of the amorphous matrix was reduced, which was similar to the phenomenon reported by Concustell et al. [28].

The mechanism of CT remains unclear up to now. Some researchers [29] have proposed that structural relaxation may be one of the microscopic mechanisms responsible for the variations in the macroscopic properties and microstructure after CT. However, Zaichenko et al. [30] has pointed out that the influence of structural relaxation is negligible at low temperatures since its intensity I is determined by the expression:

$$I \sim \exp\left[-\frac{U_i}{kT}\right] \quad (1)$$

where U_i is the mean value of the energy barrier, k is the Boltzmann constant and T is the temperature. As demonstrated above, the effect of CT on the $Cu_{46}Zr_{46}Al_8$ composite may be explicated from the following aspects: the effect on the glass matrix and the effect on the crystalline distributed in the matrix. Free volume is

defined as that part of the thermal expansion, or excess volume which can be redistributed without energy changes and the free volume theory has been used in the glass formation [31,32]. According to the literatures [16,33], the share band initiation in glassy alloys is related to free volume coalescence and the shear bands form just in the higher free volume fraction. However, it is well known that the diffusion of the free volume is related to the temperature [10,16]. In the cryogenic condition, increased stiffness of the atomic bond makes the squeezed free volume coalescence more difficult, since the mobility of the free volume at cryogenic temperature is much lower that that at room temperature. The coalescence of the free volume requires a higher applied load which results in the improvement of the microhardness and the compression strength [16,34]. Furthermore, the lower free volume leads to the fewer shear bands and suppress the propagation of the share bands. Thus, the brittle fracture was accelerated, as seen in Fig. 5. The effect of CT on the crystalline could be explained that the cryogenic condition can effectively slow down the mobility and the diffusion of atoms [10], and consequently suppress the growth of the crystalline phases, contributing to the smaller size of the crystalline phase. The martensitic phase was also induced by the internal stress during CT, which was in accord with the previous study [35]. Furthermore, the internal stress induced by CT can crumble the crystalline phase and thus lead to the smaller crystalline phases and the modification of the morphology of the CuZr phase [36]. In the crystalline materials, the relation of strength to the grain size is followed by the Hall–Pecth formula:

$$\sigma_s = \sigma_i + k_y d^{-1/2} \quad (2)$$

where σ_i and k_y are constants at a certain temperature and a certain stain velocity, and d is the diameter of the crystalline phase. Assuming the Hall–Pecth formula is also applicable in the crystalline phase of the BMG composites, it can be concluded that the smaller size of the crystalline phase results in the higher strength of the composites. Therefore, the effect of CT on the modifications of the matrix and the crystalline phase contributes to the superior hardness and the compression fracture strength to those of the as-cast samples.

CT can improve the strength and the hardness of the $Cu_{46}Zr_{46}Al_8$ composite but accelerate the brittle fracture. However, for the actual applications, the materials with high strength and large plasticity are desirable. Although CT may open a new strategy to fabricate the high-strength structural materials in the future, the details of the ductile to brittle transition at the cryogenic environment are still unclear and need further study.

4. Conclusions

In this work, the effects of CT on the microstructure evolution and mechanical properties were studied. CT refined the primary CuZr phase, induced the martensite phase and modified the morphology of the CuZr precipitates in the as-prepared Cu-based bulk metallic glasses matrix composite ($Cu_{46}Zr_{46}Al_8$), contributing to the improvement in the microhardness and the compression fracture strength from 512 Hv and 1340 MPa to 574 Hv and 1759 MPa, respectively before and after CT. The size of the CuZr crystalline phase was reduced from about 3 μm to 2 μm and the morphology of the CuZr precipitate was transformed from the rotundity to the short rod-shape. Furthermore, CT accelerated the fracture morphology transition from the ductile to the brittle. CT may be a novel way to achieve the microstructural refinement and the strength as well as microhardness improvement of the BMG composites.

Acknowledgment

The authors gratefully acknowledge the financial support of the National Natural Science Foundation of China (No. 50804015).

References

[1] J. Eckert, J. Das, K.B. Kim, Intermetallics 14 (2006) 876–881.
[2] F. Jiang, D.H. Zhang, L.C. Zhang, Mater. Sci. Eng. A 467 (2007) 139–145.
[3] D.V. Louzguine, A. Inoue, Philos. Mag. Lett. 83 (2003) 191.
[4] J. Eckert, J. Das, S.K. Roy, J. Non-Cryst. Solids 353 (2007) 3742–3749.
[5] T. Zhang, A. Inoue, Mater. Trans. JIM 39 (1998) 1001.
[6] D.H. Xu, B. Lohwongwatana, G. Duan, Acta Mater. 52 (2004) 2621.
[7] T.L. Cheung, C.H. Shek, J. Alloy Compd. 434–435 (2007) 71–74.
[8] A. Inous, W. Zhang, Mater. Trans. 43 (11) (2002) 2921–2925.
[9] P. Yu, H.Y. Bai, M.B. Tang, W.L. Wang, J. Non-Cryst. Solids 351 (2005) 1328–1332.
[10] Y.J. Huang, J. Shen, J.F. Sun, Mater. Sci. Eng. A 498 (2008) 203–207.
[11] B.Q. Zhang, Y.Z. Jia, S.T. Wang, J. Alloy Compd. 468 (2009) 187–190.
[12] S. Pauly, G. Liu, G. Wang, Acta Mater. 57 (2009) 5445–5453.
[13] J. Das, S. Pauly, J. Eckert, J. Alloy Compd. 483 (2009) 97–101.
[14] Y.F. Sun, C.H. Shek, F.S. Li, Mater. Sci. Eng. A 479 (2008) 31–36.
[15] S. Pauly, J. Das, J. Eckert, Scr. Mater. 60 (2009) 431–434.
[16] A. Kawashima, Y.Q. Zeng, M. Fukuhara, Mater. Sci. Eng. A 498 (2008) 475–481.
[17] H. Li, K. Tao, C. Fan, Appl. Phys. Lett. 89 (2006) 041921.
[18] H. Li, C. Fan, K. Tao, Adv. Mater. 18 (2006) 752–754.
[19] V.Z. Bengud, E.D. Tabachnikova, J. Miskuf, J. Mater. Sci. 35 (2000) 4449.
[20] D.W. Xing, Y.J. Yang, J. Shen, Mater. Lett. 62 (2008) 44–46.
[21] F. Jiang, Z.B. Zhang, L. He, J. Sun, J. Mater. Res. 21 (2006) 2638–2645.
[22] G. Subhash, J.R. Dowding, L.J. Keczkes, Mater. Sci. Eng. A 33 (2002) 334.
[23] P. Yu, H.Y. Bai, Mater. Sci. Eng. A 485 (2008) 1–4.
[24] L.H. Dai, Y.L. Bai, Int. J. Impact Eng. 35 (2008) 704–716.
[25] Z.F. Zhang, J. Eckert, L. Schultz, Acta Mater. 51 (2003) 1167–1179.
[26] Z. Bian, G. He, G.L. Chen, Trans. Nonferrous Met. Soc. China 10 (2000) 345.
[27] Q.S. Zhang, H.F. Zhang, Z.Q. Hu, Acta Metall. Sinica 38 (2002) 835–838.
[28] A. Concustell, S. Mato, T.G. Woodcock, Intermetallics 13 (2005) 1214–1219.
[29] S.G. Zaichenko, N.S. Perov, A.M. Glezer, J. Magn. Magn. Mater. 297 (2000) 215–216.
[30] S. Zaichenko, S. Rpth, A. Glezer, J. Magn. Magn. Mater. 571 (2003) 258–259.
[31] D. Turnbull, M.H. Cohen, J. Chem. Phys. 34 (1) (1961) 120–125.
[32] F. Spaepen, Acta Mater. 25 (1977) 407–415.
[33] K.M. Flores, R.H. Dauskardt, Acta Mater. 49 (2001) 2527–2537.
[34] R. Huang, Z. Suo, J.H. Prevost, W.D. Nix, J. Mech. Phys. Solids 50 (2002) 1011–1027.
[35] G.Z. Ma, D. Chen, Y. Jiang, W. Li, Intermetallics 18 (2010) 1254–2157.
[36] O. Shigeo, Heat Treat. 39 (1) (1999) 12–15.